

What is the most appropriate scan timing for intraoperative detection of malignancy using ^{18}F -FDG-sensitive gamma probe? Preliminary phantom and preoperative patient study

Tatsuya HIGASHI,* Tsuneo SAGA,* Takayoshi ISHIMORI,* Marcelo MAMEDE,* Koichi ISHIZU,*
Toru FUJITA,* Takahiro MUKAI,* Seiji SATO,** Hironori KATO,** Yoshio YAMAOKA,**
Keiichi Matsumoto,*** Michio SENDA*** and Junji KONISHI*

*Department of Nuclear Medicine and Diagnostic Imaging, Kyoto University Graduate School of Medicine

**Department of Gastroenterological Surgery, Kyoto University Graduate School of Medicine

***Department of Image-based Medicine, Institute of Biomedical Research and Innovation

Purpose: To evaluate the appropriate post-injection timing for hand-held-gamma-ray-detecting probe (GDP) scanning for the intraoperative detection of malignancy after preoperative F-18 FDG (FDG) injection. **Methods:** Patient study with superficially located cancer was performed on three patients before operation by dual-phase whole-body PET at 2 and 6–7 hr post-injection of FDG (370 MBq), and by probe scanning from the skin at several points at 1, 3, 5, and 7 hr after FDG injection. TNRa (tumor-adjacent-normal ratio) and TNRc (tumor-contralateral-normal ratio) were calculated. Phantom study was also performed to determine basic GDP function. **Results:** The patient study revealed that tumors showed constant TNRa (0.9–1.3) and TNRc (1.1–3.0) by GDP count rate, and that there was no tendency of an increase in TNRa with time. The standard deviations of GDP count rate were lower at 1–3 hr post-injection compared with those of delayed scans. While delayed PET showed an increase or no change in the tumor FDG uptake, the decrease of normal tissue FDG uptake was not adequate to create higher TNRs. The phantom study revealed that LN model showed TNRa of 1.7 or greater by GDP count rate (cps) when background contained no FDG, but that they showed TNRa of 1.3 or less when the background contained 4% of the LN FDG activity per ml. **Conclusion:** The present study suggests that higher FDG count rate of tumors at 1–3 hr post-injection would be more suitable for the gamma-probe detection compared with lower count rate at 6–7 hr delayed scans with wide standard deviations.

Key words: gamma-detecting probe, F-18 fluorodeoxyglucose, tumor-to-normal ratio, positron emission tomography, post-injection time

INTRODUCTION

INTRAOPERATIVE USE of gamma-detecting probe (GDP) has been widely used for the detection of sentinel lymph node of breast cancer, melanoma, and other malignancies.^{1–4} For the detection of sentinel lymph node, low energy-

gamma-emitters, such as technetium, have been used for the labeling of colloids. Recently, some studies reported that GDP may also contribute to the intraoperative detection of malignancy after preoperative IV injection of F-18 labeled fluoro-2-deoxy-D-glucose (F-18 FDG), positron emitter with high energy-gamma-ray.^{5–7} Compared with the sentinel lymph node detection after in-site-injection of radioactive colloid, in which the radioactive colloid flows just along the local lymphatic system without high background activity, the GDP detection of F-18 FDG accumulation is complicated by high background activity since F-18 FDG is administered intravenously and distributes to normal tissue in addition to malignant lesions. Previous studies showed the feasibility of F-18 FDG-

Received March 5, 2003, revision accepted November 21, 2003.

For reprint contact: Tatsuya Higashi, M.D., Department of Nuclear Medicine and Diagnostic Imaging, Graduate School of Medicine, Kyoto University, 54 Shogoin-kawahara-cho, Sakyo-ku, Kyoto 606–8507, JAPAN.

E-mail: higashi@kuhp.kyoto-u.ac.jp

guided intraoperative detection of malignancy at one hour post injection, but these results provided only a relatively low tumor-normal ratio (TNR).⁵⁻⁷ Recently, some studies revealed that delayed scan of F-18 FDG PET is useful in the differentiation of malignancy in patients with head & neck cancer and pancreatic cancer because of higher TNRs obtained at the delayed scan.^{8,9} Considering the decrease in the F-18 FDG uptake in the normal tissues and the increase or persistent trapping in the malignant tumor with time, probe-scanning at delayed timing, such as 2 hr or greater after injection of F-18 FDG might be more useful compared with the scan at 1 hr after injection. However, no study has evaluated the appropriate timing for the GDP scanning after IV injection of F-18 FDG. The aim of the present study was to evaluate the advantages and disadvantages of the tumor-detection by the GDP at the delayed timing after F-18 FDG injection and to elucidate the appropriate timing for the intraoperative GDP tumor detection. We conducted a preoperative clinical study in patients with superficially located tumors using sequential GDP tumor detection at 1–7 hr and using dual-phase FDG PET. To confirm the data achieved in the patient study, we also conducted an additional phantom study simulating a superficially located tumor model.

MATERIALS AND METHODS

Gamma Detecting Probe and FDG

The gamma-detecting probe (GDP) used in the present study was a CXS-OPSZB with the Crystal Probe System 2000 model (Crystal GmbH, Berlin, Germany, distributed by Anzai Medical Co., Tokyo, Japan). The detector portion of the instrument is a hand-held device measuring 22 mm in diameter with a PET collimator designed for high energy gamma ray and containing a CsI: Tl scintillator with Si photo-diode for detection of radioactivity.¹⁰ In the present study, only one energy window setting (430–511 keV) was used for the detection of F-18 FDG. Radioactivity measurements were taken over 1-second and/or 10-seconds periods. All the results shown in the present study were calculated at each time point as the average of 4-times counting for 1-second and as the average of 2-times counting for 10-seconds.

Patients

The present study group comprised 3 patients (3 females; mean age, 56 yr; age range, 34, 54, 80 yr) with a superficially located malignant lesion. Surgical resection or needle biopsy confirmed the histological diagnosis, as 2 cases of invasive ductal adenocarcinoma of the breast (pt #1, 3), and one case of Virchow's lymph node metastasis from adenocarcinoma of the stomach (pt #2). Before being enrolled in this study, each patient gave written informed consent, as required by the Kyoto University Human Study Committee.

FDG-PET Imaging and Probe Detection

F-18 was synthesized by the nucleophilic substitution method with an F-18 FDG-synthesizing instrument, F-100 (Sumitomo Heavy Industries, Co. Ltd., Tokyo, Japan) and a cyclotron, CYPRIS-325R (Sumitomo Heavy Industries, Co. Ltd., Tokyo, Japan).¹¹ For image acquisition, a whole-body PET was performed using GE Advance (General Electric Medical System, Milwaukee, WI, distributed by GE-Yokogawa Medical Co., Tokyo, Japan) that had a single detector ring 512 BGO, which provides 35-slice acquisitions per frame with 4 mm width and a spatial resolution of 5 mm (FWHM). The patients fasted for at least 5 hr before the F-18 FDG injection. Patients were injected 74 (pt #1) or 370 (pt #2, 3) MBq of F-18 FDG, and studied by dual-phase whole-body F-18 FDG PET at 2 hr and 6–7 hr after the injection. Five frames of static emission scanning were performed for 3 min per frame to obtain the image from the face to upper thigh. For attenuation correction, transmission scanning was performed immediately after the emission scans for 1 min per frame. For image reconstruction, ordered subsets expectation maximization (OSEM) was performed with the use of segmented attenuation correction (SAC). Standardized uptake values (SUVs) of the tumor and normal tissues (heart, liver, muscle, and urinary bladder and region contra-lateral to the main tumor) were determined for each time point. Each patient also received probe scanning from the skin surface at more than 20 points in the body at 1, 3, 5, and 7 hr or 1, 3, and 6 hr after F-18 FDG injection. At each point, the standard deviation (SD) and the coefficient of variation (C.V.) were also calculated to evaluate the fluctuation of GDP count rate by the 1-second counting. C.V. (%) were determined as follows;

$C.V. (\%) = SD \text{ (of 4-time counting at each point)} \div \text{the average count rate (cps)} \times 100.$

Tumor-normal ratios (TNRs) were defined using two methods as TNRa (tumor-adjacent-normal ratio) and TNRc (tumor-contralateral-normal ratio).

Probe Sensitivity Measurement

The basic performance of this GDP was evaluated and confirmed for sensitivity and linearity by the distributing company and by our institute in the range from 37 KBq (1 μ Ci) to 74 MBq (2,000 μ Ci), and in the distance from –15 cm to 15 cm horizontally or in the distance from 0 cm to 30 cm vertically. To check the spatial characteristics of relative sensitivity of this GDP, a point source of F-18 FDG was measured with the GDP positioned upright in the air at various positions. This experiment was performed as in Table 1, which showed the relative sensitivity of the GDP count rates at various distances (0–32 cm) from the point source of F-18 FDG (74 MBq/2 mCi) in vertical, horizontal and 45° directions.

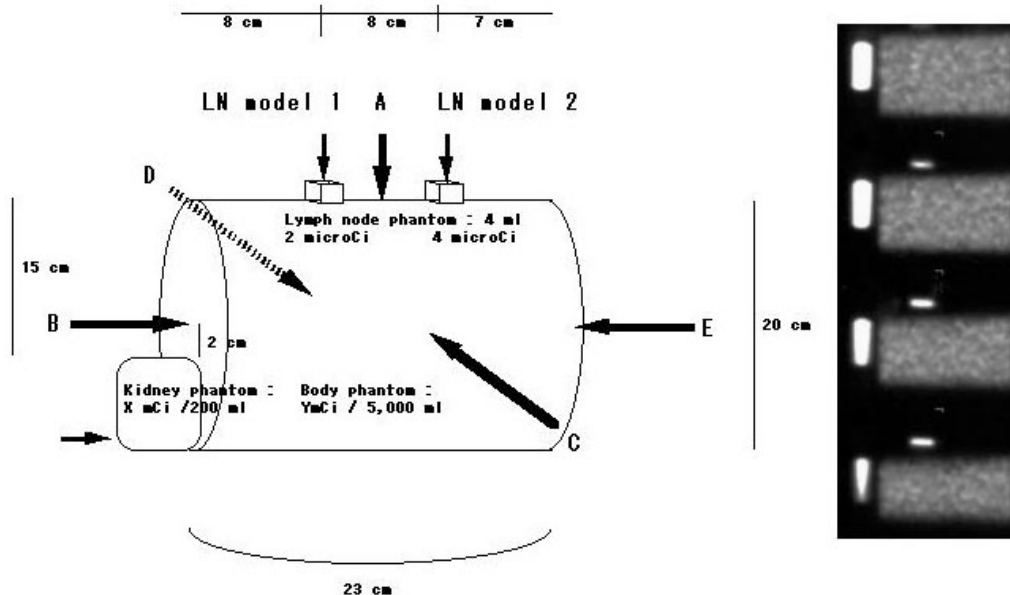
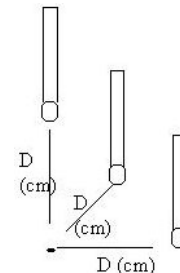


Fig. 1 Schematic figure of the phantom used in the present study. It consists of a saline-filled 5.0-liter-plastic-barrel as the “Body trunk,” with a saline-filled 0.2-liter-plastic-bottle as a critical organ (“Kidney”), and with two 4-mL-nodules (“LN models 1 and 2”) made of saline-soaked absorption paper wrapped with plastic wrapping paper. Probe scanning was performed at each point, as shown in this Figure at 1, 2, 3, 4, and 6 hr after the F-18 FDG injection. PET images of the phantom with activity in “LN model 2,” “Body trunk” and “Kidney,” obtained by a whole-body PET machine, are also shown at 4 slices on the right.

Table 1 Relative sensitivity as a function of the probe distance and direction from a point source



Direction of probe to source with radioactivity (74 MBq)	Distance from point source (D)						
	0 cm	1 cm	2 cm	4 cm	8 cm	16 cm	32 cm
vertical direction	1.00	0.54	0.42	0.31	0.14	0.05	0.01
horizontal direction	0.71	0.37	0.27	0.14	0.05	0.02	0.00
45 degree direction	0.49	0.32	0.25	0.12	0.04	0.01	0.00

Phantom Study

For the phantom study, a saline-filled 5.0-liter-plastic-barrel was designed as the “Body” with uniform background activity that was attached with a saline-filled 0.2-liter-plastic-bottle representing an organ with high F-18 FDG uptake, such as the “Kidney” (Fig. 1 left). At each probe study, both of them contained different doses of F-18 FDG inside (Table 2), as follows;

“Body”: 0, 7.4, 14.8, or 37 MBq (0, 0.2, 0.4, 1.0 μ Ci),

“Kidney”: 0, 3.7, 7.4, 14.8, or 37 MBq (0, 0.1, 0.2, 0.4, 1.0 mCi).

Two 4-mL-nodules with 74 and 148 KBq (2 and 4 μ Ci) of F-18 FDG (“LN model 1 & 2”) (dose fixed), made of saline-soaked absorption paper wrapped with plastic wrapping paper, were also attached to the barrel to simulate the superficially located tumor nodules. The distance between “LN model 1 or 2” and “Kidney” was approximately 17 or 22 cm, respectively. Probe scanning from the surface was performed at 9 points in the phantom, as follows; 1 point each for “LN model 1 and 2” and 1 point for “Kidney,” 5 points for “Body” (A–E) and 1 point for background (Fig. 1 left). Tumor-normal ratio (TNR) was

Table 2 Results of GDP count rates in lymph node, body and kidney model with different radioactivity in body and kidney

Kidney Phantom: X mCi		0.0	0.1	0.2	0.4	1.0	0.0	0.1	0.2	0.4	1.0	0.0	0.1	0.2	0.4	1.0	0.0	0.1	0.2	0.4	1.0
Body Phantom: Y mCi		Body Phantom: 0 mCi					Body Phantom: 0.2 mCi					Body Phantom: 0.4 mCi					Body Phantom: 1.0 mCi				
Kidney model	average	0	181	354	666	891	25	323	365	706	917	30	288	372	690	940	93	258	361	680	921
	SD	0	18	14	14	24	4	8	33	24	14	4	16	8	18	29	10	24	12	22	35
LN model 1 (2 microCi)	average	23	26	26	30	37	49	55	56	62	74	102	101	99	108	108	190	193	201	214	226
	SD	5	3	6	5	3	5	7	5	9	7	6	2	4	12	10	16	23	13	12	11
TNRa		1.9	2.1	1.7	1.8	1.8	1.5	1.5	1.1	1.1	1.2	1.1	1.2	1.1	1.2	1.3	1.0	1.0	1.1	1.1	1.1
LN model 2 (4 microCi)	average	39	37	42	43	39	74	74	72	85	79	121	113	107	113	105	210	210	197	188	235
	SD	4	4	8	8	6	10	8	11	9	7	5	10	13	9	4	7	16	5	10	17
TNRa		3.3	3.0	2.6	2.5	1.8	2.2	2.0	1.4	1.5	1.3	1.3	1.3	1.2	1.3	1.3	1.1	1.1	1.0	1.0	1.1
Background																					
A	average	12	12	16	17	21	33	37	51	58	62	90	85	89	87	83	186	194	191	192	209
	SD	2	3	3	4	3	4	4	1	14	8	12	3	6	12	10	18	16	10	7	11
B	average	1	50	117	154	357	49	159	256	328	316	74	170	206	333	375	176	264	265	480	535
	SD	0	7	9	10	25	5	12	9	9	11	7	12	15	24	21	14	19	19	25	39
C	average	1	3	5	12	17	52	57	64	60	58	84	88	91	102	87	179	190	190	206	215
	SD	0	1	2	3	2	2	11	6	5	4	13	6	9	5	7	5	25	14	7	7
D	average	1	4	7	12	28	61	50	60	58	59	96	94	95	93	97	190	200	211	205	229
	SD	0	2	2	5	7	2	3	5	5	8	8	7	14	11	7	11	26	6	5	8
E	average	1	3	4	6	9	40	49	54	46	57	81	75	71	88	84	169	170	160	168	170
	SD	0	2	2	2	4	6	6	7	4	3	11	10	7	10	3	7	15	13	9	11

defined as TNRa (tumor-adjacent-normal ratio), which was calculated as count rate of the “LN model” divided by those of point A.

PET image acquisition was also performed by a whole-body PET machine using this phantom with F-18 FDG of 18.5 MBq (0.5 mCi) in the “Body,” 11.1 MBq (0.3 mCi) in the “Kidney,” and 0.148 MBq (4 μ Ci) in the “LN model 2” (Fig. 1 *right*). Methods of image acquisition were almost the same as in the human study, mentioned above.

RESULTS

Basic Study of the Probe

The results of radioactivity measurements were compared between the count rates (cps) over the 1-second period and those over the 10-second period at the same point, and showed that the averaged ratio of count rates between the 10- to 1-second periods (10-1-ratio) remained fairly constant at all the points as calculated with the value of 10.93 ± 1.55 (average \pm SD). Therefore, the results given below were examined using the GDP count rates (cps) over the 1-second period.

Table 1 shows the relative sensitivity in the GDP count rate at the time of the vertical move from the point source with various directions of the GDP head. This table revealed that 70–50% of the original count rates could be detected at the horizontal or 45 degree direction of the GDP head directly attached to the source, which means the inefficiency of lateral gamma-ray shielding of this probe. At the horizontal or 45-degree distance of 8 cm from the pin source, the count rates would indicate almost

5% of the original count rates.

Phantom Study

Table 2 shows the GDP count rate at each point at the time of each dose setting for the phantom. Without radioactivity in either the “Kidney” or “Body,” the count rates measured by GDP at the site of the “LN model 1 & 2” (23 and 39, respectively) were “true count rates.” In this condition, the count rate at background point A was a mixture of the horizontal count rates (4 cm) from the “LN model 1 & 2,” which could be calculated as about 14% of the “true count rates” of the “LN model 1 & 2” as shown in Table 1. With any dose of F-18 FDG in the “Body,” there was no significant effect on the count rate of the “LN model 2” by an increase in the “Kidney” dose, probably due to the distance of 22 cm. On the other hand, the count rates of the “LN model 1” and the background point A showed an increase in relation to the increase in the “Kidney” dose, probably due to the shorter distance of 17 cm. According to Table 1, greater than 1% of the “Kidney” count rate would be added to the true “LN model 1” count rates. TNRa showed a relatively high value of 1.7 or greater in every case without F-18 FDG in the “Body.” However, TNRa showed quite a low count rate with a value of 1.3 or less in every case with an F-18 FDG dose of 0.4 (4% of the LN activity per ml) or greater in the “Body.”

Phantom images obtained with a whole-body PET machine are shown in the right hand portion of Figure 1. SUVs were measured as 1.10 for the “Body,” 15.46 for the “Kidney,” and 5.78 for the “LN model 2,” which means

Table 3 Results of the quantitative analysis using SUV in the dual-phase FDG-PET

Patient		first PET		second PET	
		(hr after injection)			
		SUV			
		Max in ROI	Average in ROI	Max in ROI	Average in ROI
#1	Breast ca.	2 hr		7 hr	
	Main tumor (breast ca., left)	11.3	5.0	12.8	6.7
	contralateral side (right)	0.8		0.7	
	heart	31.3	10.6	21.7	12.9
	liver	2.1	1.4	2.9	1.3
	muscle	7.2		3.9	
	kidney	2.9	1.7	1.9	0.7
	urinary bladder	20.2	11.5	5.2	3.0
#2	Gastric ca. Post-ope./Virchow LN metastasis	2 hr		6 hr	
	Main tumor (Virchow LN, left)	9.4	5.1	11.0	6.0
	contralateral side (right)	2.0		1.7	
	heart	3.9	2.0	5.6	2.2
	liver	2.9	2.0	2.8	1.9
	muscle	1.0		1.6	
	kidney	15.0	2.8	8.7	1.5
	urinary bladder	56.3	22.6	71.9	35.6
#3	Breast ca.	2 hr		7 hr	
	Main tumor (breast ca., left)	8.1	3.1	5.6	2.2
	contralateral side (right)	0.1		0.1	
	heart	6.2	3.0	3.9	1.6
	liver	2.7	1.7	1.9	1.2
	muscle	3.1		3.9	
	kidney	10.9	1.8	8.5	1.5
	urinary bladder	17.3	11.5	17.4	10.2

TNRa by FDG-PET images was 5.25 although TNRa by GDP count rates showed only 1.2–1.3 in a similar situation (Table 2).

Patient Studies

Table 3 summarized the results of dual-phase F-18 FDG PET, in which overtime changes of SUVs in the various positions of the bodies of Patients 1–3 are shown. Tumor uptake was consistently high even in the 6–7 hr delayed scans in all cases. Table 3 also shows that the changes in the SUVs were quite variable in the normal tissues and that there was no tendency for a one-way decrease in the F-18 FDG uptake in the normal tissues. In Patient 1, most of the normal organs showed a decrease in the F-18 FDG uptake, while the heart showed an increase. In Patient 3, however, the uptake in the muscles, contra-lateral side of the breast and urinary bladder showed almost no change, while that in the heart showed a decrease. In Patient 2, the F-18 FDG uptake of the tumor, urinary bladder, heart and

muscle showed rises, while the contra-lateral side of the supraclavicular fossa and liver showed almost no change. Comparisons between the 2 hr and 6 hr images of the F-18 FDG PET for Patient 2 are shown in Figure 2.

Temporal change of the count rates of tumors and normal background examined by GDP was basically consistent with the decay of F-18 FDG (Fig. 3). Figure 4 shows a comparison of TNR between GDP count rates and PET images, which shows that the TNRc examined by GDP were relatively lower than the TNRc calculated by SUVs. TNR by GDP count rates were consistently low between 1.0–1.3 both in TNRa and TNRc, except for the TNRc for Patients 1 and 3. The overtime changes observed in the TNRc examined by GDP were not always compatible with the overtime changes in the TNRc calculated by SUVs. Furthermore, even for each value at each time point, TNR calculated by SUVs in the PET study did not show a close relation with the results of TNRs by GDP count rates, which implies that GDP count rates were

Table 4 Coefficient of variation (%) of GDP count rates at each scan point in patient study

GDP Scan time	Patient #1				Patient #2			Patient #3			
	Injected dose: 74 MBq				Injected dose: 370 MBq			Injected dose: 370 MBq			
	1 hr	3 hr	5 hr	7 hr	1 hr	3 hr	6 hr	1 hr	3 hr	5 hr	7 hr
Location	C.V. (%)				C.V. (%)			C.V. (%)			
rt neck (carotid A)	6.2	22.5	17.2	45.6	1.5	5.6	13.6	2.4	6.3	9.6	13.6
lt neck (carotid A)	17.1	18.2	29.7	32.5	6.5	6.1	13.7	3.8	6.5	8.0	11.7
rt axilla	16.2	25.7	23.4	31.5	5.4	6.0	23.2	3.1	10.0	7.8	13.8
lt axilla	13.1	15.9	21.2	48.1	6.2	8.4	12.5	4.6	5.9	8.4	10.8
rt upper abd	15.1	28.3	37.8	28.6	0.9	10.0	7.4	2.4	8.9	8.0	11.2
lt upper abd	12.9	17.2	19.6	42.6	2.9	2.8	28.3	1.9	7.7	11.3	5.7
center of the upper abd	15.9	35.8	24.5	72.0	4.3	3.8	13.3	2.2	10.0	15.7	13.5
center of the mid abd	15.9	32.1	36.0	44.5	6.6	6.3	11.1	3.5	6.8	4.3	19.7
center of the lower abd	7.9	9.0	24.2	47.8	7.2	5.0	9.6	5.9	9.9	11.2	7.8
rt inguinal (femoral A)	3.9	8.2	33.7	20.2	5.2	4.3	9.5	5.8	2.1	10.5	5.1
lt inguinal (femoral A)	17.9	35.3	11.2	45.7	5.4	2.5	10.0	6.0	6.5	6.8	5.1
Main tumor	18.2	12.0	33.2	25.3	4.1	3.5	16.0	3.9	4.2	9.1	18.9
Average of all the points	13.4	21.7	26.0	40.4	4.7	5.3	14.0	3.8	7.1	9.2	11.4

Table 5 Estimation of FDG distribution in a patient with the weight of 50 kg injected of 10 mCi of FDG 2 hr before

	Total weight (gram = ml)	Average SUV	radioactivity (microCi)
Total body	50,000	1	5,000
Heart	250	10	250
Liver	1,200	2	240
Kidney	100	2	20
Urinary bladder	200	15	300
Lymph node	2	10	2

affected by other factors, such as the presence of nearby organs with high-activity of F-18 FDG.

Evaluation of the Fluctuation of Count Rates

Table 4 shows that the overtime change in the C.V. of the count rates at several normal points and the superficially located tumors in each patient. At all the locations in Patients 2 and 3, the C.V. showed lower values of 10% or less at 1–3 hr compared with those at 5–7 hr after F-18 FDG injection. Considering the low F-18 FDG dose administered to Patient 1, the 1 hr after injection in this case corresponded to the 5 hr measurement in the other two patients. In Patient 1, most of the locations showed a C.V. higher than 10%.

DISCUSSION

One of the problems for the accurate detection of malignant nodules by GDP after IV injection of F-18 FDG is that there is relatively high background activity from

surrounding soft tissues and from nearby organs, such as the brain, heart, kidney and urinary bladder. It would be preferable to have a high tumor-normal ratio (TNR) for the better intraoperative detection of the malignancy by GDP. However, the present results of TNRs examined by GDP were relatively low although the TNRs of “true activity” measured by SUVs in PET at each point were sufficiently high in the present study. Although our findings of GDP in the patient study were obtained by indirect touch to the lymph nodes or the breast cancers through the skin, previous intraoperative studies showed compatible results with those of the present study by direct touch to lymph nodes with GDP. They reported a tumor-normal ratio (TNR) of less than 3.0 detected with an F-18 FDG-guided probe for the intraoperative detection of malignancy in many cases.^{5–7} According to the present findings, these poor TNRs were partially due to the relatively high-activity level of background soft tissues surrounding the tumor, but also due to the presence of high-activity organs located nearby in the body-trunk. For the establishment of an intraoperative tumor-detection system using F-18 FDG-guided GDP, it is necessary to have a method to alleviate the high F-18 FDG activity both in the background soft tissues and in the nearby organs located in the body-trunk.

First, high activity in the background soft tissues should be considered. It was expected before this study that there might be a constant decrease in the radioactivity in the normal organs and background tissues despite stable or increased uptake in the tumor, resulting in an increase in TNRs with time. However, the present results using this experimental system showed that TNRs were fairly stable in GDP count rates and showed almost no change between early and delayed FDG-PET during the entire observation

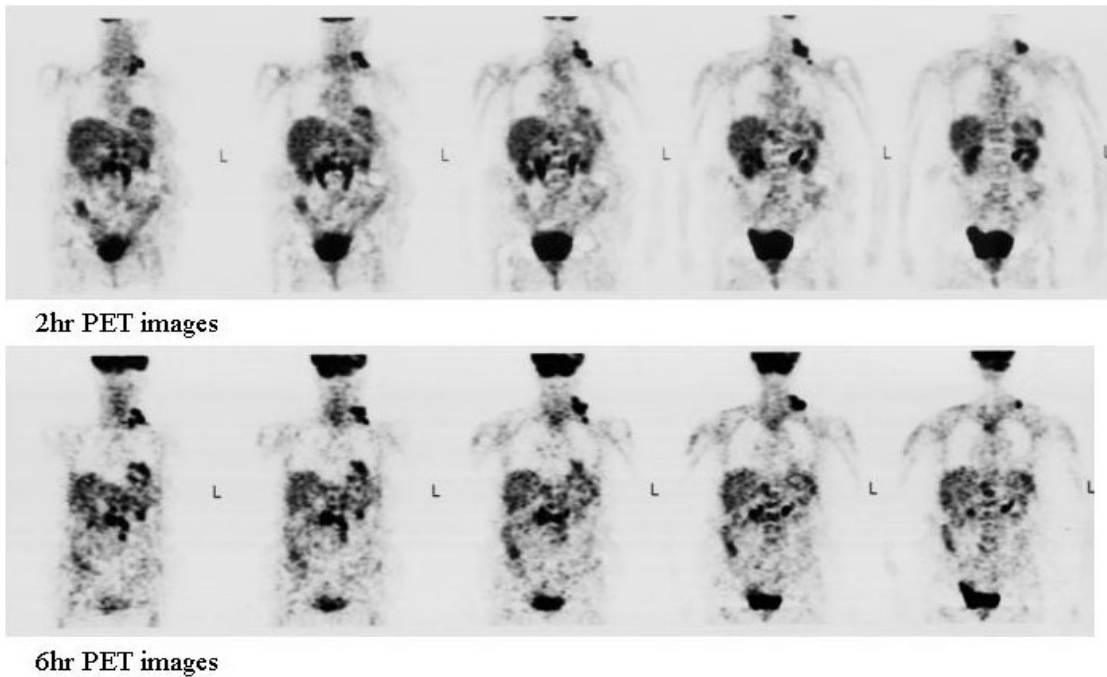


Fig. 2 Comparison between the 2 hr and 6 hr F-18 FDG PET whole-body images of patient 2. The image quality at 6 hr was coarser than that at 2 hr, but basically there was no significant difference in the F-18 FDG uptake of any organ between 2 hr and 6 hr images, including the uptake of the tumor. Note the disappearance of the bilateral kidney uptake, and the change in the shape in the heart and colon uptake in the 6 hr images.

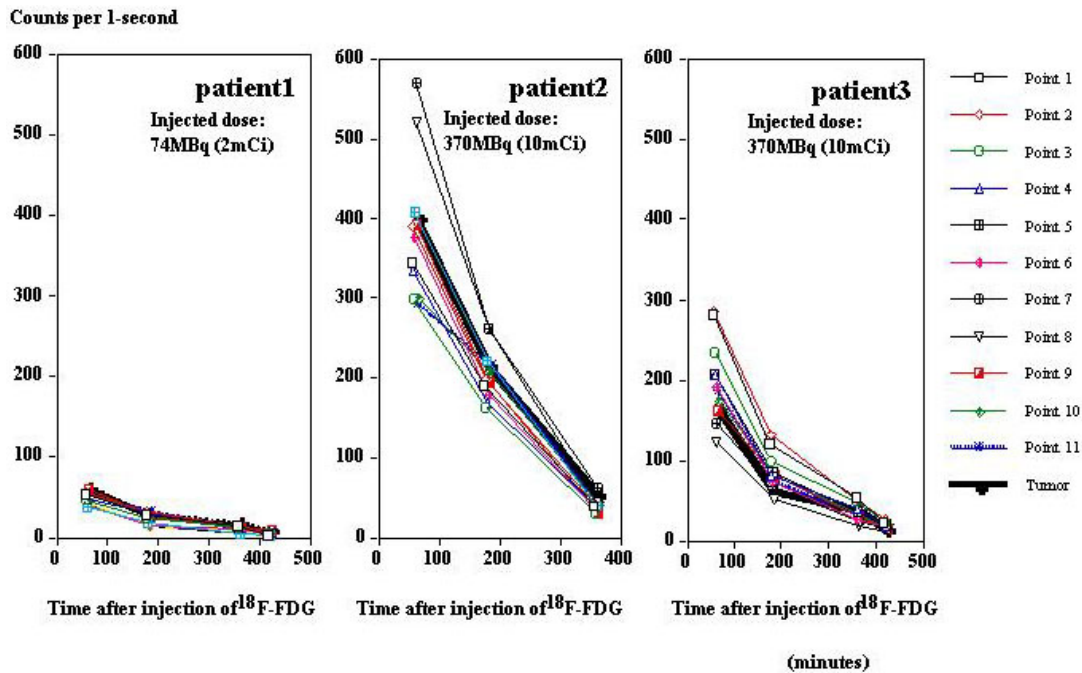


Fig. 3 Time course of count rates at each probe scanning point in each patient. Count rates from all points showed a steady decrease, which was compatible with the decay in the F-18 FDG.

time up to 7 hr. Furthermore, the results of TNRs calculated by GDP count rates and those by SUVs of PET did not show a good correspondence. This suggests that the

GDP results did not correctly represent the real activity. The increase in TNRc for Patient 1 was considered to be unreliable because it was not compatible with the results

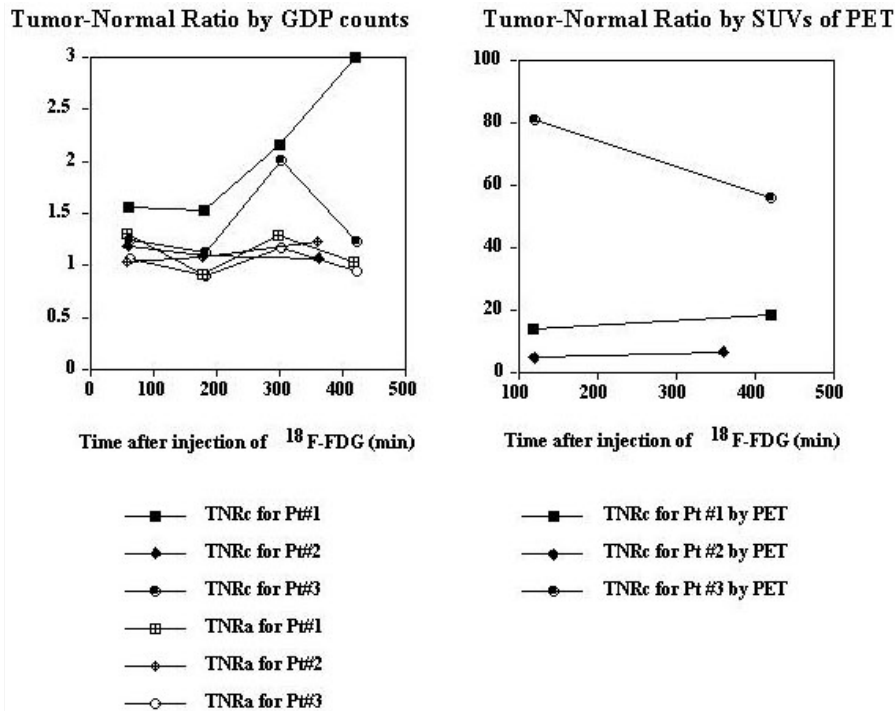


Fig. 4 Time course of the tumor-to-normal ratio (TNRa and TNRC) of the patients for whom the GDP count rate (*left*) and SUV (*right*) of tumors were calculated. Most of them appeared fairly steady during the entire study period, except for the TNRC for Patients 1 and 3. Note the difference in the values of the y-axis. There was a significant difference in TNR between GDP count rates and SUVs at each time point.

of SUVs in the PET study. Rather, this overtime change was due to the false rise from the relatively wide fluctuation of count rates due to the decay in the F-18 FDG. As a means of the alleviation of high activity in the background soft tissues, the delayed GDP scanning was not useful. These results in the present study suggest that the lower F-18 FDG count rates of tumors in the 6–7 hr scans after the injection due to physical decay would be problematic for the gamma-probe detection because of the unstable counting results even if there is some gain in the true tumor/background ratio in the late phase. Table 4 shows that the detection at 1–3 hr after F-18 FDG injection was the most reliable without a wide fluctuation in the count rates. The present findings suggest that the most appropriate probe scan timing for the intraoperative detection of malignancy is approximately 1–3 hr after F-18 FDG injection when 370 MBq is used for the injection dose. If we use a lower dose of FDG for this purpose, we could have only 1–2 hours for transfer of the patient from the RI facility to an operation room and for laparotomy procedure after injection of FDG in an RI facility, because FDG injection is only permitted in a designated RI facility in Japan.

Second, the high activity in nearby organs should be considered. It is inevitable for the intraoperative GDP detection in the abdominal/pelvic cavity to have these high-activity organs located nearby, such as the heart,

kidney, liver, and urinary bladder. For example, the para-aortic lymph nodes are located within 10 cm from either of the kidneys with high F-18 FDG activity. Table 1 shows that at the horizontal or 45 degree distance of 8 cm from the pin source, the count rates would indicate almost 5% of the original count rates. If these results were obtained in water filled condition, the relative sensitivity would be much smaller than those in the present study. However, the space between the para-aortic lymph node and the kidney would be free air when an intraoperative GDP detection is performed. Therefore, our data in Table 1 are basically adequate for intraoperative GDP detection. Table 2 also shows that the distance of 17 cm between the “LN model 1” and the “Kidney” was not adequate for the accurate counting of the “true activity” for the “LN model 1,” even in the water filled condition. Both of these results imply that count rates of a superficially located mass surrounded by high activity organs are not “true count rates” from the target mass and are strongly influenced by the high-activity organs. It was initially suggested that alleviation of the high activity in these organs would be the most desirable aspect for the intraoperative GDP tumor detection and delayed counting would be feasible for the alleviation. Even in the 6–7 hr delayed PET, however, some of these organs showed no change or increase in their remaining F-18 FDG activities. If FDG activity of the surrounding mass could not be alleviated,

it appears that the volume of the high-activity mass would be critical for accurate and effective intraoperative GDP detection. It is necessary to consider the volume and activity of the surrounding organs.

Table 5 shows a simplified simulation of the distribution of F-18 FDG in a 50 kg person who was injected with 370 MBq (10 mCi) 2 hr previously. If it is assumed that this person has a volume of 50-liter (50,000 ml), in which 5,000 μ Ci of F-18 FDG is basically homogeneously diffused, and if the volumes of the heart, liver, kidney and urinary bladder are assumed to be 250, 1200, 100, and 200 ml and the average SUV of these organs as 10.0, 2.0, 2.0, and 15.0, respectively, the total radioactivity of these organs would be approximately 250, 240, 20, 300 μ Ci. If these organs are located within 8 cm of the target mass in the peritoneal cavity, the radioactivity of the mass would be measured by GDP as the real activity plus 5% of about 2000, 2000, 1000, 2500 counts per second, respectively (according to our results, not shown). In addition, if the volume of the mass with an SUV of 10.0 (for example, the lymph node in the intra-peritoneal cavity) is 2 ml (= 2 g), this suggests that the mass would be measured by GDP as the real count rates of about 30 counts per second on the background count rates of about 50–125 by the surrounding organs. Figure 1 shows the PET images obtained by PET scanner for a phantom model with “Body,” “Kidney” and the “LN model 2,” based on the estimation of Table 5. In this figure, the “Body,” “Kidney” and the “LN model 2” containing 500, 30 and 2 μ Ci of F-18 FDG in the volume of 5000, 20 and 2 ml were measured as SUVs of about 1.0, 15 and 10. According to this estimation in the present experimental system, it is admittedly quite difficult to accurately detect F-18 FDG uptake of intra-peritoneal small lymph node by intraoperative use of GDP, although the PET images in Figure 2 show clear TNRa.

Therefore, in order to avoid the influence of the high activity in nearby organs, it is necessary to improve the collimation and to thicken the lateral shielding of this type of GDP for the use of intraoperative detection of malignancy. However, the weight and size of the collimator attached to the GDP would be problematic when the high energy gamma ray of F-18 (511 keV) is considered. If lead (Pb) is used for the lateral shielding against F-18, shielding cover wall of Pb with 3.8 mm thickness would be needed for half-value layer. In order to have a 1/8- or 1/16-value layer for semi-complete shielding, a 12 mm or thicker shielding cover wall of Pb would be needed for the probe head, which would be too heavy for handling. In terms of physics, tumor detection using GDP is always difficult because of the lack of lateral shielding of high energy gamma ray of F-18 (511 keV). Further technical advances would be needed.

Table 5 also shows the importance of the alleviation of the background soft tissue activity. If the phantom in the present study represents the body trunk with a volume of 5,000 ml, an SUV = 1.0 or lower would be critical for the

GDP count rates, because it means approximately 500 μ Ci of F-18 FDG contained in the phantom, as shown in the right hand portion of Figure 1. Table 2 shows that TNRa was relatively low with a value of 1.3 or less in every case with an F-18 FDG dose of 400 μ Ci or greater in the “Body.” Therefore, it is necessary to have a background soft tissue activity lower than an SUV of 0.8–1.0 for the GDP counting. The results in the patient PET study (Table 3) showed that SUVs of the normal tissue in the contralateral side of the tumor varied from 0.1 to 2.0. These findings suggest that the relatively high background F-18 FDG activity influenced GDP count rates somehow at least in Patient 1 and 2.

In summary, the present findings of the phantom and patient studies showed that intraoperative detection of an intra-abdominal small mass using GDP would be influenced by the surrounding high F-18 FDG activity not only in the background soft tissues but also in the nearby organs located in the body-trunk. Although all of these activities varied from high to low in each patient, there was no consistent decrease in the radioactivity in the normal organs and background tissues with time at least in this experimental model. Therefore, it is not necessary to wait for a decrease in the F-18 FDG activity in the normal tissues for 6–7 hours, and the most appropriate probe scanning timing for the intraoperative detection of malignancy would be around 1–3 hr after F-18 FDG injection.

One limitation of this study was that this is not a real intraoperative study. As mentioned above, our findings of GDP counting in the patient study were performed in the non-invasive condition and by indirect touch to the lymph nodes or the breast cancers. Direct touch to the malignant lesion in the intraoperative condition could improve the TNRs; however, the results of the previous intraoperative studies were basically similar to our findings. Two patients (1 and 3) were outpatients, not resting on a bed, who sometimes walked around. If the patients were kept at rest, supine-positioned in bed and fully hydrated by glucose-free solution, the uptake of the heart, urinary bladder, and muscles could be decreased, but the effect of this intervention is unclear. In patient 2 who rested in a wheel chair with hydration by glucose-free solution during the entire study, the F-18 FDG activity of bilateral kidney showed a significant decrease with time, while those of the heart, ureter and urinary bladder showed increases. Further evaluations using a resting position and an intensive hydration procedure are required.

CONCLUSION

The present findings suggest that 1) GDP detection using F-18 FDG of superficially located tumors was strongly affected not only by the high-activity background, but also by other high-activity nearby organs, even with a distance of 10 cm or greater, and could not provide a high

tumor-normal ratio (TNR), and 2) the higher F-18 FDG count rates of the tumor of 1–3 hr scans after the injection would be easier for the gamma-probe detection without a wide standard deviation, compared with the lower count rates of 6–7 hr delayed scans with wide standard deviations.

ACKNOWLEDGMENT

The authors thank Anzai Medical Co. for their assistance with our research.

REFERENCES

1. Alazraki NP, Styblo T, Grant SF, Cohen C, Larsen T, et al. Sentinel node staging of early breast cancer using lymphoscintigraphy and the intraoperative gamma detecting probe. *Radiol Clin North Am* 2001; 39 (5): 947–956.
2. Dubois RW, Swetter SM, Atkins M, McMasters K, Halbert R, et al. Developing indications for the use of sentinel lymph node biopsy and adjuvant high-dose interferon alpha-2b in melanoma. *Arch Dermatol* 2001; 137 (9): 1217–1224.
3. Tsavellas G, Patel H, Allen-Mersh TG. Detection and clinical significance of occult tumour cells in colorectal cancer. *Br J Surg* 2001; 88 (10): 1307–1320.
4. Ramires PT, Levenback C. Sentinel nodes in gynecologic malignancies. *Curr Opin Oncol* 2001; 13 (5): 403–407.
5. Desai DC, Arnold M, Saha S, Hinkle G, Soble D, et al. Correlative whole-body FDG-PET and intraoperative gamma detection of FDG distribution in colorectal cancer. *Clin Positron Imaging* 2000; 3 (5): 189–196.
6. Zervos EE, Desai DC, DePalatis LR, Soble D, Martin EW. F-18 labelled fluorodeoxyglucose positron emission tomography-guided surgery for recurrent colorectal cancer: a feasibility study. *J Surg Res* 2001; 97 (1): 9–13.
7. Essner R, Hsueh EC, Haigh PI, Glass EC, Huynh Y, et al. Application of an F-18 fluorodeoxyglucose-sensitive probe for the intraoperative detection of malignancy. *J Surg Res* 2001; 97 (1): 120–126.
8. Hustinx R, Smith RJ, Benard F, Rosenthal DI, Machtay M, et al. Dual time point fluorine-18 fluorodeoxyglucose positron emission tomography: a potential method to differentiate malignancy from inflammation and normal tissue in the head and neck. *Eur J Nucl Med* 1999; 26 (10): 1345–1348.
9. Nakamoto Y, Higashi T, Sakahara H, Tamaki N, Kogire M, et al. Delayed FDG PET Scan for Differentiation Between Malignant and Benign Lesions in the Pancreas. *Cancer* 2000; 89 (12): 2547–2554.
10. Vogt H, Bachter D, Buchels HK, Wengenmair H, Dorn R, et al. Sentinel lymph node detection by preoperative lymphoscintigraphy and intraoperative gamma probe guidance in malignant melanoma. *Nuklearmedizin* 1999; 38 (4): 95–100.
11. Kitano H, Magata Y, Tanaka A, Mukai T, Kuge Y, Nagatsu K, et al. Performance assessment of O-18 water purifier. *Ann Nucl Med* 2001; 15 (1): 75–78.